

Technologies for cold cathode field electron emission, a review

Jake Skelton, supervised by Andrew Jardine

30th April 2021

Abstract

Field emission is the phenomenon whereby electrons tunnel through a material's surface potential barrier if subjected to a large electric field. Devices based on this principle have potential as electron sources that are smaller, faster and more efficient than thermionic emitters, and that can operate at room temperature. In this paper, we review the historical development of field emitters, their inherent benefits and drawbacks, the applications for which field emission would be most appropriate, and the challenges still to overcome.

1 Introduction

The generation of free electrons is absolutely integral to modern physics experiments - from particle accelerators to microscopes. And yet, most of today's electron sources are close cousins of the cathode ray tube with which J.J. Thomson discovered the electron, in 1897. The principle driving these devices is *thermionic emission*, or liberating electrons from a solid filament by heating it to over 1000K and supplying a current. Thermionic emitters have undergone enormous improvements over the decades, in current density, work function, size, and noise to name but a few metrics. And for a time they formed the primary building block of information technology, in 'valves' or 'vacuum tubes'. But thermionic emitters suffer a handful of fundamental limitations; the high temperatures required can be an issue in itself, but also makes thermionic emission power intensive and inefficient. The sluggish response of hot cathodes is another problem - emission current must be modulated by a tertiary grid electrode rather than at the source.

Field electron emission, in which electrons subject to a large electric field tunnel through a solid's surface potential, started to gather serious interest as an alternative to thermionic emission in the 1970s. The theory of the phenomenon was initiated by Fowler and Nordheim in 1928, but it took developments in vacuum technology and microfabrication to make field emission (FE) a viable electron source. In practice, the strong fields needed are achieved using sharp-tip cathode geometries. Beginning with the

work of C. Spindt and colleagues, prototypes of large arrays of Mo and Si FE tips became increasingly sophisticated up to the close of the 20th century, driven in large part by the interest in replacing cathode ray tube (CRT) electron sources in televisions and computer displays. The chief draws of field emitter arrays (FEAs) were their small size, their speed, the ability to address individual FE tips, and their ease of manufacture.

After the discovery of carbon nanotubes (CNTs) - generally attributed to Iijima in 1992 - these quickly became an object of interest to FE researchers. Their very high aspect ratio, and chemical stability made them promising emitter candidates. Over the next decade, researchers continued to improve carbon, metal, and semiconductor FE prototypes and techniques, but commercial implementations were very rare. After the mid 2000s however, the possibility of field emitter displays (FEDs) becoming a commercial reality became increasingly clouded by manufacturing difficulties, and the success of liquid crystals and light emitting diodes (LEDs) in this sphere. Avenues for practical FE research do remain: in particular, for microwave amplification, but also electron microscopy, x-ray generation, radiation-resistant electronics and even space propulsion.

Following this brief introduction, this review examines the different theoretical electron-emission regimes, and the most widely-used technologies in section 2. Section 3 discusses the more mature FE substrates, while section 4 examines carbon nanotubes - their production, characteristics, and challenges. Section 5 outlines the most promising potential applic-

ations of FE, and finally section 6 offers concluding remarks.

2 Background

In this section, we briefly discuss field emission theory in the context of thermionic and Schottky emission, and then go on to profile the alternatives to thermionic emission which have already seen some adoption.

2.1 Theories of electron emission

For electrons to leave a solid, they must overcome the surface potential (SP) barrier; at large distances this is the classic *image charge* potential [1]. This can be achieved by thermal excitation of the electrons, or by applying an electric field of such strength that the SP becomes narrow enough for electrons to tunnel through. The applied field also reduces the height of the SP somewhat, so it can be used in concert with thermal excitation. The first process is thermionic emission, and is described by the Richardson-Dushman exponential relationship [2]; the second is field emission, and the third is known as the *Schottky effect*. These phenomena are shown schematically in fig 2.1.

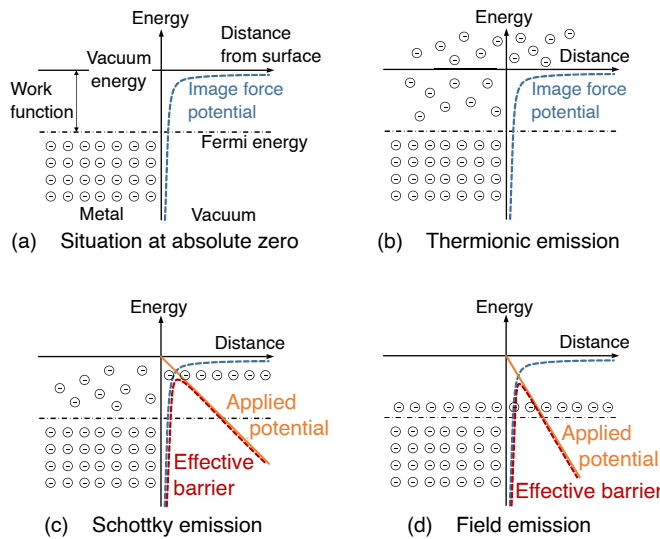


Fig. 2.1: Schematic representation of the difference between a) a cold metal surface, b) thermionic emission, c) Schottky emission, and d) field emission. Note the $1/x$ image potential and the effect of a linear applied field. Adapted from [3]

In 1928, Fowler and Nordheim applied the Wentzel-Kramers-Brillouin approximation and newly-minted Sommerfeld theory to a model with a triangular SP ('FN theory') [4]. The form of their

equation, linking the current density J with the applied field E is, in S.I. units

$$J(\phi, E) = \frac{e^3}{16\pi^2\hbar} \frac{\mu^{1/2}}{(\phi + \mu)\phi^{1/2}} (\beta E)^2 \exp\left(-\frac{4}{3e}\sqrt{\frac{2m}{\hbar^2}} \frac{\phi^{3/2}}{\beta E}\right) \quad (1)$$

where ϕ is the material's work function, μ is its Fermi energy, and $-e$ and m are the electron charge and mass, respectively. β is the *field-enhancement factor* and is determined by emitter geometry: sharp features amplify applied fields in accordance with classical electrostatics [5]. Commonly, (1) is put into the straight line form

$$\ln\left(\frac{I}{V^2}\right) = A - \frac{B}{V} \quad (2)$$

where I is the emission current, V is the applied voltage, and A and B are parameters which depend on ϕ , T and other practical details.

Strictly, (1) equation applies only to metals, but (2) is encountered in experimental current-voltage measurements of a variety of substrates so it is often taken as a hallmark of FE. An example experimental plot is shown in fig 2.2. Discussions of the subtleties of FE theory can be found in [2, 6, 7], but we do not pursue them here.

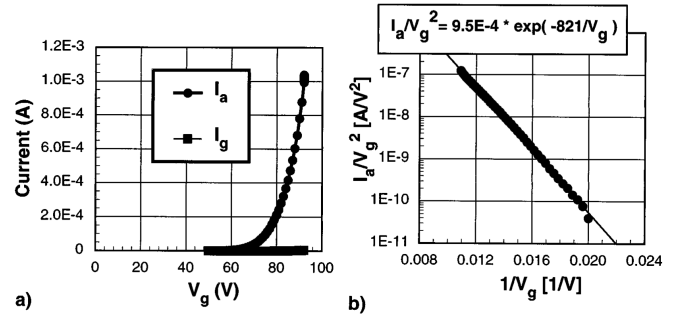


Fig. 2.2: Experimental field emission data. (a) linear-linear plot showing the FN exponential relationship, (b) Fowler-Nordheim plot. Reproduced from [8].

2.2 Dominant emission technologies

It is the author's view that experimental FE prototypes must be placed in the context of the current electron emitter state-of-the-art. Thermionic emitters have not been totally replaced in any field where free electrons are used, but some other technologies have seen uptake.

Typical thermionic emitter operating parameters are cathode temperatures in the range 1000 to 3000 K, DC current densities around 10 A/cm^2 (and higher in pulsed-mode), and lifetimes of several thousand hours when operated at typical vacuums of 10^{-8} mbar [6]. Single-tip sources based on the

Schottky effect are popular in electron microscopy and lithography. Almost always made from W and ZrO, they can achieve exceptional brightnesses of $10^4 \text{ A cm}^{-2} \text{ V}^{-1}$ (total emission $\sim 100 \mu\text{A}$) and are typically operated at $\sim 1500 \text{ K}$ and 10^{-9} mbar [6, 9]. Also popular in microscopy are FE sources with a single W tip - 'cold cathode tungsten' (CCW). These are valued for their small source size but typical currents are $100\times$ smaller than Schottky emitters'. As will be explained in section 3, CCW emitters suffer from gas adsorption and ion sputtering in operation, and so require vacuums of 10^{-10} mbar [9, 10]. Fig 2.3 shows a selection of electron micrographs of these technologies.

For completeness, we mention a further emission technique popular in accelerator physics. Photoemission, based on the photoelectric effect explained by Einstein, is valued for its control over the time of electron pulses, and electron momentum and polarisation. In this context, FE is usually seen as an irritating source of noise [11], but some groups are considering it as an alternative to photoemission for power-constrained accelerators and synchrotrons [12, 13].

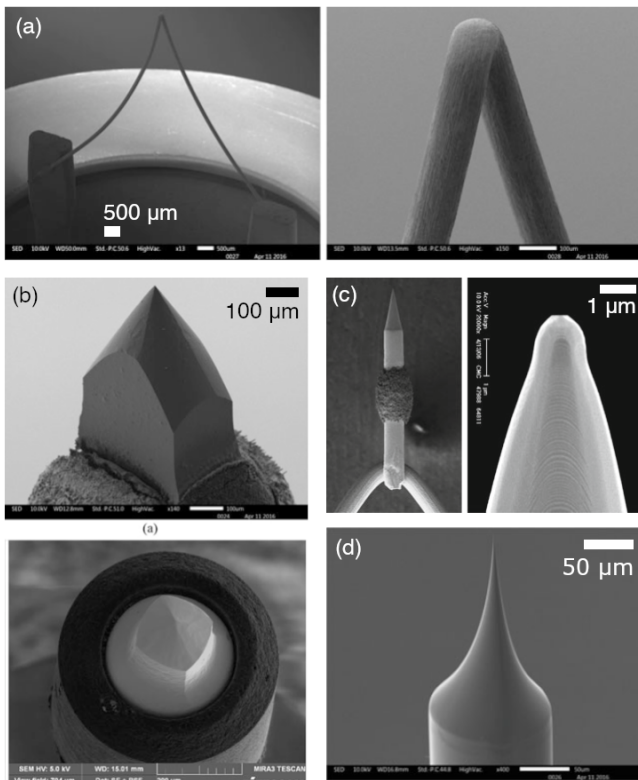


Fig. 2.3: SEM images of four electron emitters in commercial use. (a) (top two panels) shows a twisted W thermionic cathode. (b) (left two panels) shows two lanthanum hexaboride thermionic cathodes. (c) shows a W/ZrO Schottky emitter. (d) shows a cold cathode W field emitter. Panel (c) is adapted from [6]; the remainder from [9].

3 Metal and semiconductor field emitters

3.1 Spindt field emitter arrays

Although FE had been used as an imaging technique in surface physics since its discovery [14], early attempts to use it as an electron source, based on etched wires, were plagued by short lifetimes and high voltage requirements [15]. In his first paper on the topic, in 1968, C. Spindt presented a small number of Mo tips in a field emitter array (FEA) that could emit $6 \mu\text{A}$ for a week without degradation [16]. A SEM image from this work is shown in fig 3.1a.

Now, 'Spindt array' has come to denote an array of metal (usually Mo) tips, separated from a surrounding gate electrode by a layer of insulator, forming a diode. Fig 3.1 shows several examples. The general process for manufacture of a Spindt emitter is outlined in fig 3.2; for more detail see [14].

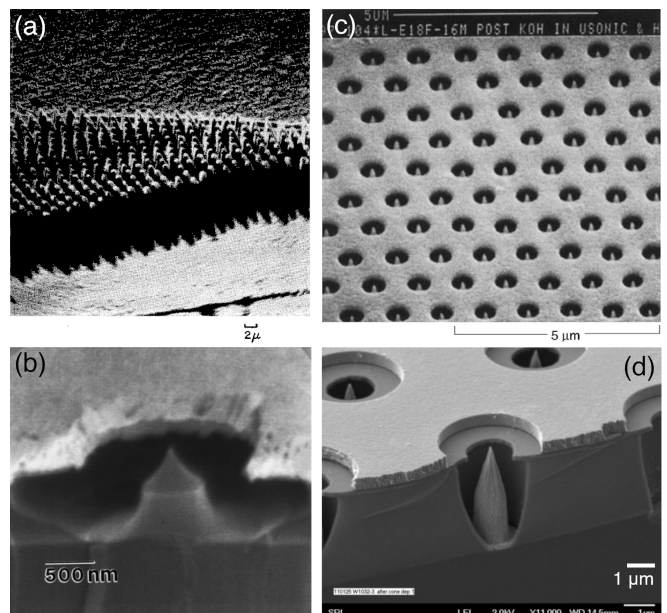


Fig. 3.1: Electron micrographs of four different molybdenum Spindt arrays. (a) is the first reported field emitter array. Note that (c) has a scale bar showing a gate pitch of about $1 \mu\text{m}$. Adapted from (a) [16], (b) [8], (c) [17] (d) [18].

A selection of experimental data for Spindt arrays are shown in table 3.1, otherwise, operating parameters are pressures of 10^{-9} mbar and room temperature. Generally, an array of fewer tips necessitates greater tip current to be useful and thus larger current densities are reported. Current densities as high as 10^3 A/cm^2 can be achieved with techniques to create very small gate spacings, such as laser interferometry [14].

Tips	I_{tip} (μA)	J (A/cm^2)	V (V)	Reference
100	100	278	326	[19], 2015
50,000	6	40	160	[20], 2004
50,000	2	15	75	[21], 2009

Table 3.1: Select Spindt FEA data. I_{tip} is the tip current, J is the current density, and V is the cathode-gate voltage.

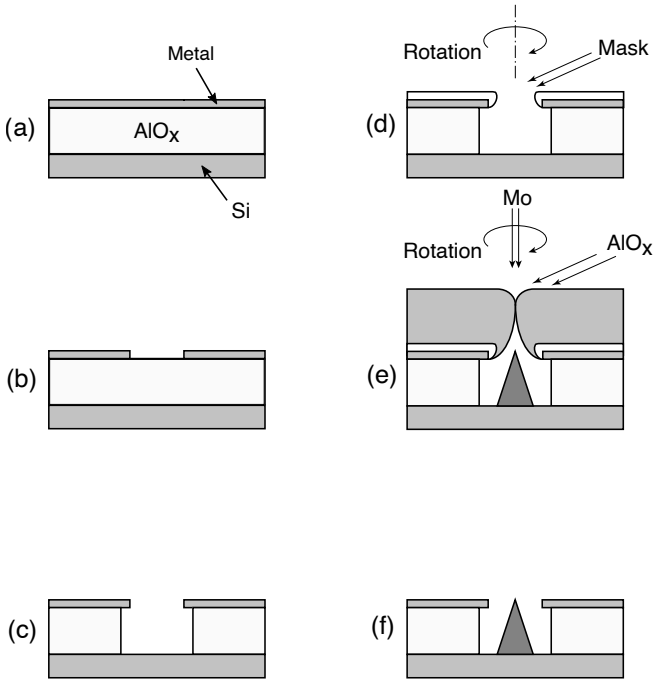


Fig. 3.2: Fabrication of a Spindt FEA. (a) A sandwich of a metal (to form the gate) on insulator, on a silicon substrate is created using e-beam evaporation deposition. (b) An array of holes is bored into the metal using lithography. (c) Insulator is chemically etched out from under the hole. (d) A mask is deposited onto the metal surface by spraying with e-beam deposition from an oblique angle, while the sample is rotated. (e) Aluminium oxide (for example) is deposited likewise; simultaneously, Mo is deposited normally via e-beam deposition. (f) Finally, the mask is etched away to reveal the tip. Adapted from [14].

The emission signal from Spindt FEAs is inherently noisy. Besides the omnipresent shot noise of individual electrons, fluctuations in emitted current are caused by three types of processes. (i) *Ion sputtering*: the strong electric field involved can accelerate positive ions in the vacuum chamber toward the cathode. The collision causes a 'blip' in emission and can cause individual tips to fail. (ii) Adsorption of gases onto the cathode. Naturally, this can be mitigated with improved vacuums. (iii) FE is dependent on atomic-scale emitter geometry; transitions of individual atoms can create 'bistable' noise, an example of which is shown in fig 3.3. In single-tip emitters like CCW, these effects are very undesirable, hence the ultra-high vacuums mentioned in section 2.2; the accumulation of adsorbed gases is mitigated by 'flashing the tip' - heating it over 1000 K for a few minutes periodically without applied voltage [9]. In FEDs, the

major impetus for FEA development, noise from individual tips could be mitigated by using more tips, or by implementing ballast resistors in the Si substrate, and so less research has been done on noisy Spindt tips.

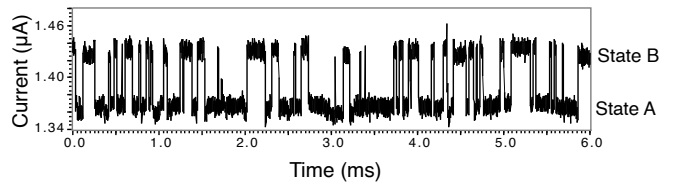


Fig. 3.3: Bistable noise from a Spindt field emitter. The peak-to-peak amplitude is about 1 μA which represents 5% of the total current. Adapted from [14].

3.2 Silicon field emitter arrays

From the start, Spindt arrays were constructed with microfabrication techniques, so naturally there was interest in creating FEAs from silicon. Thomas *et al.* reported the first practical realisation in 1972 [22]. Si FEAs are fabricated using a plethora of available semiconductor etching, deposition and lithography techniques; a detailed discussion of the benefits of each is beyond the scope of this article but a typical fabrication process is outlined in fig 3.4. The wealth of Si microfabrication techniques allows advanced circuitry to be constructed around each emitter, including multiple gate electrodes, and, in the silicon substrate, resistors, diodes, and even MOSFETs [14]. Some examples of Si emitters are shown in fig 3.5

The emission characteristics of Si FEAs are very comparable with those of Mo arrays. For example, [8] presents extensive testing of two Si FEAs, with electrical characteristics as given in table 3.2. Degradation of Si FEAs occurs by the same mechanisms as metallic emitters. There is a wealth of evidence of reduced emission current upon introduction of gases to the vacuum environment; fig 3.6 illustrates the effect of oxygen exposure. As with Mo, re-lowering the pressure for a few hours without applied voltage is sufficient to desorb gases from the emitter [23]. Arc discharge, in poor vacuum or due to micro-protrusions on emitter tips, can be a source of more catastrophic failure in semiconductor or metal gated FEs. Fig 3.7 shows the aftermath of an arc discharge event in a Si FEA.

Tips	I_{tip} (μA)	J (A/cm^2)	V (V)
28,000	0.70	2	700
18,300	0.27	2	75

Table 3.2: Silicon FEA data for two arrays, from [8]. I_{tip} is the tip current, J is the current density, and V is the cathode-gate voltage.

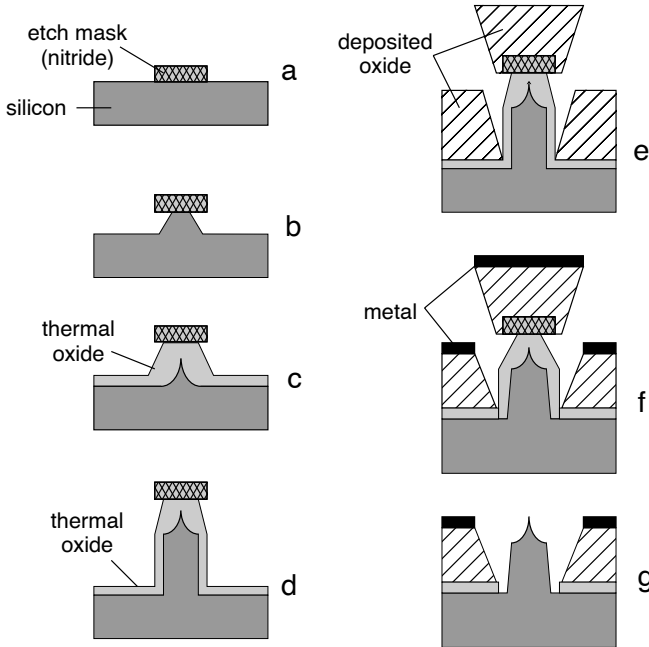


Fig. 3.4: Fabrication of a silicon field emitter array. (a) dots of nitride mask are deposited. (b) the silicon is etched, isotropically or anisotropically, leaving a stump under the mask. (c) oxidation attacks flat surfaces more than protrusions, sharpening the tip. (d) (optional) a directive etch can elongate the stump. (e) SiO_x (insulator) deposited with electron-beam techniques. (f) metal (gate) layer deposited likewise. (g) oxide etched to reveal tip. Reproduced from [14].

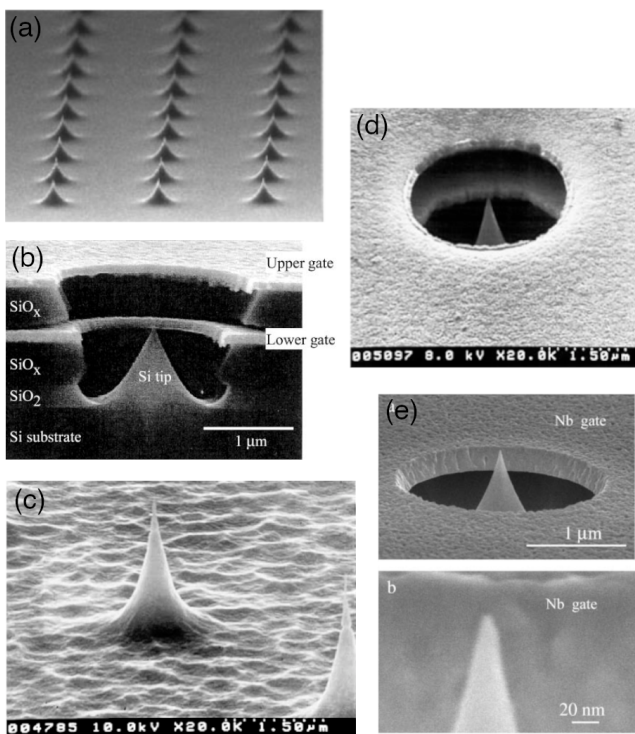


Fig. 3.5: Selection of silicon field emitters. (a) and (c) show ungated Si arrays, (e) shows an array with anode gates, and (b) and (d) show doubly gated arrays. (c) and (d) are adapted from [24], the remainder from [14].

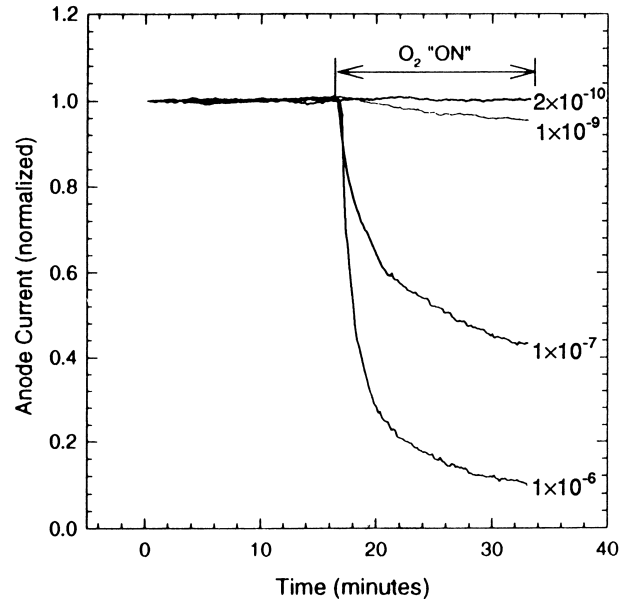


Fig. 3.6: Effect of oxygen adsorption on a Mo FEA. Four different pressures were investigated, and are shown next to the corresponding trace, in torr ($1 \text{ torr} \approx 1.33 \text{ mbar}$). Reproduced from [25].

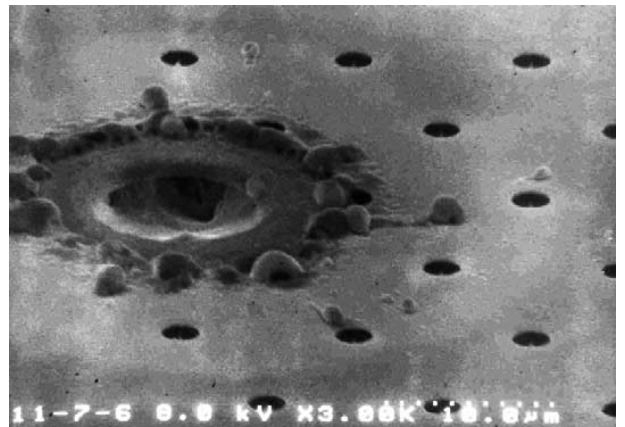


Fig. 3.7: Failure of a silicon FE tip due to arc discharge and resultant heating. Reproduced from [24].

3.3 Cold cathode tungsten and more exotic materials

As mentioned in section 2.2, individual tungsten tips are a popular emitter for electron microscopy. Thus far, CCW represents the only FE technology which has had commercial success; both Mo and Si FEAs discussed in this section have never been successfully commercialised. The popularity of CCW means there is much excellent literature on the topic, which the reader is directed to for more information [6, 9, 26, 27].

In the 1990s, there was much interest in diamond-like carbon and graphite as FE materials [14, 24]. The focus has largely switched to carbon nanotubes (CNTs), however, due to their exceptional aspect ratio and ease of production.

4 Carbon nanotubes

Four years after Iijima's discovery of carbon nanotubes [28], the first CNT field emitter was reported by de Heer *et al.* in the form of an electron gun made from a sheet of carbon nanotubes [29]. The current density was reportedly 0.1 mA/cm^2 at 200 V. These data are obviously inferior to the state of the art in Si and Mo FEAAs but, as we shall detail, CNT results soon improved. CNTs quickly drew the interest of FE researchers because of their very high aspect ratio (up to ~ 1000), and the chemical stability of carbon which was evident in diamond, graphite, and fullerenes already. Some examples of CNT FEAAs are shown in fig 4.1

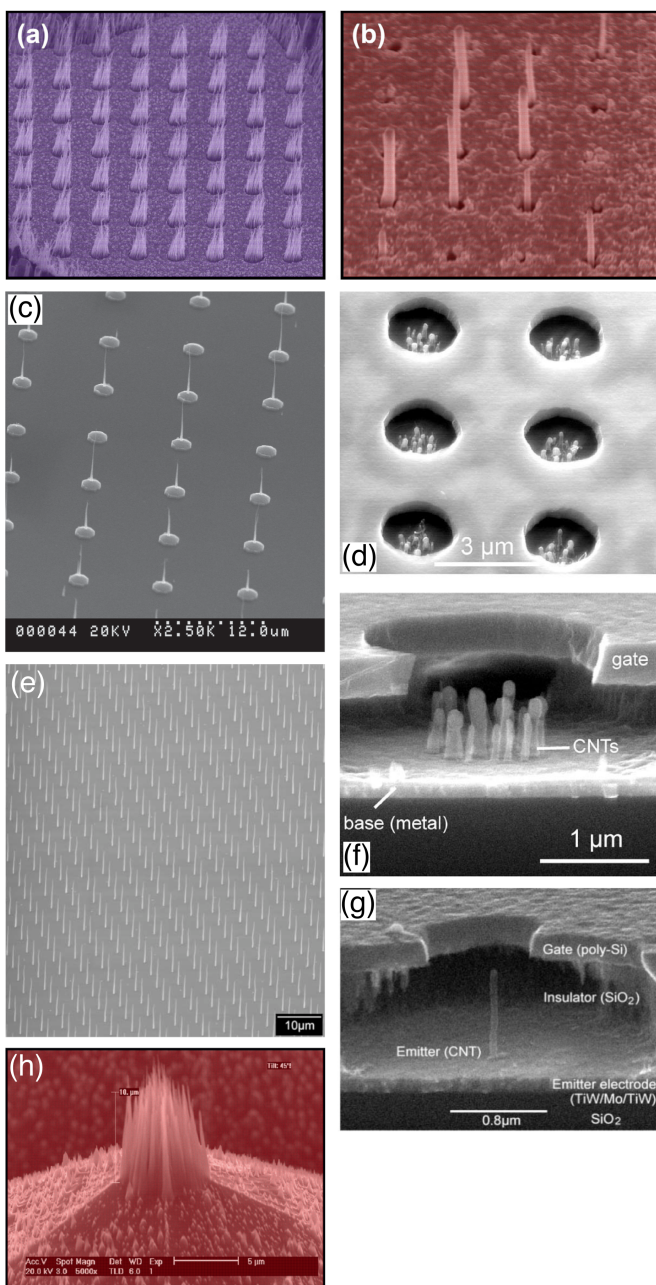


Fig. 4.1: Examples of carbon nanotube field emitters. (e) and (h) show ungated arrays, (c) shows gate electrodes at the CNTs' feet, and the remainder show a raised anode gate layer. (a, b, c) adapted from [10]. (c) from [30]. (d, f) from [31]. (e, g) from [32]

Both Iijima and de Heer's experiments made CNTs using electric arc discharge (EAD), but, currently, the most successful technique for CNTs is *chemical vapour deposition* (CVD); the process is outlined in fig 4.2. CVD has the advantages that it allows control over the placement of CNTs, and their length, is scalable, and a variant of it, plasma-enhanced CVD (PECVD), allows one to control the direction of CNT growth [10].

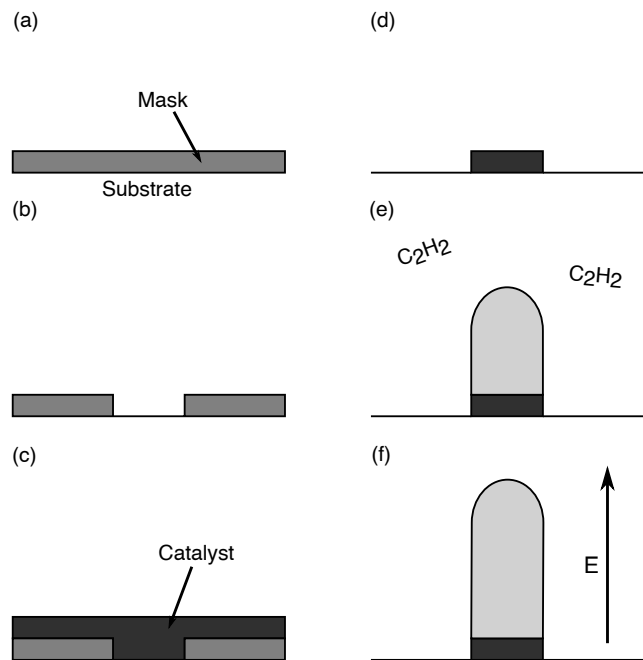


Fig. 4.2: Manufacture of carbon nanotubes via chemical deposition. (a) A photomask is deposited onto the substrate (Si, for example). (b) Photolithography (or electro-lithography for very fine spacing) is used to bore an array of holes in the mask. (c) The catalyst (often Ni) is deposited in a uniform layer. (d) Lift-off of the mask in solvent leaves 'dots' of catalyst. (e) Chemical vapour deposition (CVD) with a feedstock (often acetylene or methane) starts the growth of CNTs on the catalyst dots. (f) Plasma-enhanced CVD lowers the temperatures necessary for growth (allowing a wider range of substrates and catalysts) and using the DC applied voltage causes nanotubes to align with the field. For more information see [10].

Because CNTs are grown on a catalyst bed, and several catalysts are suitable, a large number of substrates can be used for CNT FE. Silicon, in particular, allows the construction of gate electrodes [33] and ballast resistors [34]. It is common to use an anode distant from the emitter plane too, in which case larger voltages are needed. A selection of electrical characteristics for CNT emitters are collated in table 4.1; it is clear that it is possible to achieve current densities comparable with Si and Mo FEAAs, although, to the author's knowledge, the Spindt array literature still contains the largest such values.

Density (cm^{-2})	I_{total} (mA)	J (A/cm^2)	Anode voltage (V)	Turn-on field ($\text{V}/\mu\text{m}$)	Reference
10^5	-	0.6	40 ¹	30	[33]
-	10	10	3500	6	[34]
-	-	0.001	400	1.67	[35]
-	-	0.001	800	3.16	[35]
10^6	2.5	1	-	6	[36]
10^7	10	4	-	-	[36]
-	-	0.001	-	3	[37]
10^6	0.4	4	3000	1.5	[38]
-	0.55	0.275	40 ¹	-	[30]

Table 4.1: Performance of a selection of carbon nanotube field emitters. Various constructions are included: gated, ungated, ordered array and carpeted types. I_{total} is the total supplied current, J is the current density. Note 1: these data are from gated arrays so the anode is significantly closer to the CNTs.

4.1 Performance

The issues facing Mo and Si FEAs that have prevented their commercial adoption were not related to raw current output, but rather stability and uniformity [14]. CNTs emit more stably, but improving uniformity still requires the incorporation of ballast resistors or other circuitry to restrain individual tips which are dominating the emission [10, 30, 34]. This circuitry is only possible when CNT placement is highly controlled: EAD, or CVD with a uniform bed of catalyst, produce a ‘carpet’ of nanotubes in which there is great variation in tip current. Li *et al.* made qualitative measurements of the uniformity of 11×11 and 20×20 arrays of CNTs by directing the emission at a sheet of polymethyl methacrylate (PMMA) [39]; their results are shown in fig 4.3 and demonstrate the heterogeneity of CNT FEA emission without added circuitry.

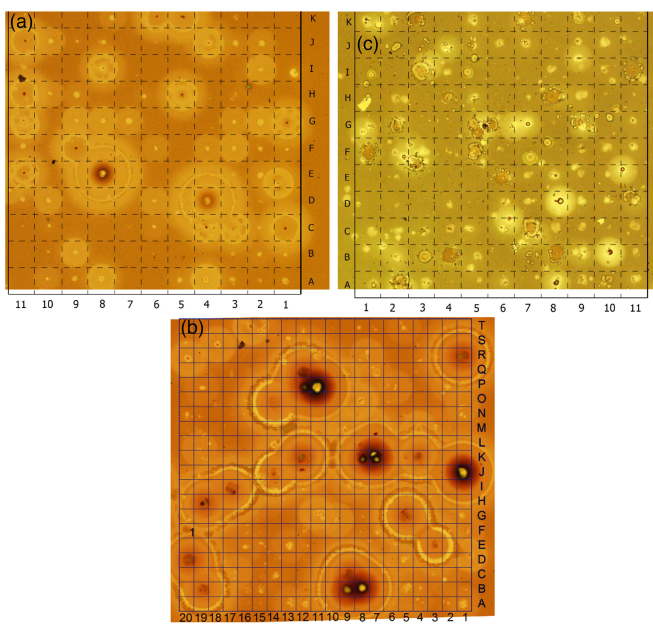


Fig. 4.3: Uniformity of emission from CNT arrays tested with a PMMA target screen. (a) and (c) depict an 11×11 array, (b) a 20×20 array. Note that if all nanotubes were emitting uniformly, there would be dots in each of the squares, of the same size. Adapted from [39].

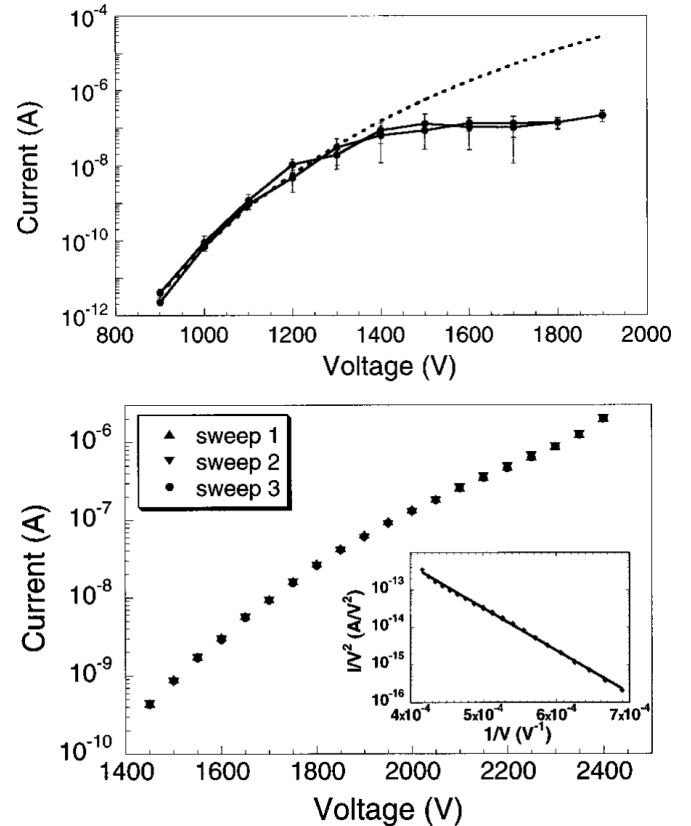


Fig. 4.4: Current saturation of CNT FE due to surface adsorbates. The top panel shows data from an unclean single CNT; the dotted line is a fit of the FN equation. The lower panel shows the result of cleaning the nanotube by heating it to 900K for several seconds. The inset is a plot in the FN form (2). Adapted from [40].

As for stability, there is a large body of evidence showing that CNT FE deviates from the FN form, (2), at high electric fields, to form a current plateau [10, 14, 34]. Dean and Chamala were the first to explain this [40]: the current saturation is due to gas molecules adsorbed onto the CNT. They found, with individual nanotubes, that saturation occurred after reaching about $2 \mu\text{A}$. Clean nanotubes, in contrast, follow the FN theory well but in fact operate at a lower current for the same voltage. This saturation is shown in 4.4. In some contexts the saturation offers a desirable stability, in contrast to the FN exponential

variation with the electric field; in other contexts, the reliability of the FN form may be preferable. It remains to be seen how consistently CNTs can be made to saturate, by changing the pressure for example.

In contrast to metal and semiconductor FEAs, the main failure mode of CNTs is not ion sputtering; the chemical stability of carbon resists this [14]. There are two primary failure mechanisms for CNTs: (i) detachment from the substrate at the foot [41, 42], and (ii) resistive heating at high current densities [42]. The latter is perhaps less pernicious because larger CNT arrays can be used to spread the current load, and the measures already described to increase uniformity assist in this also. Failure at the nanotube base is still poorly understood and there are no agreed mitigation measures.

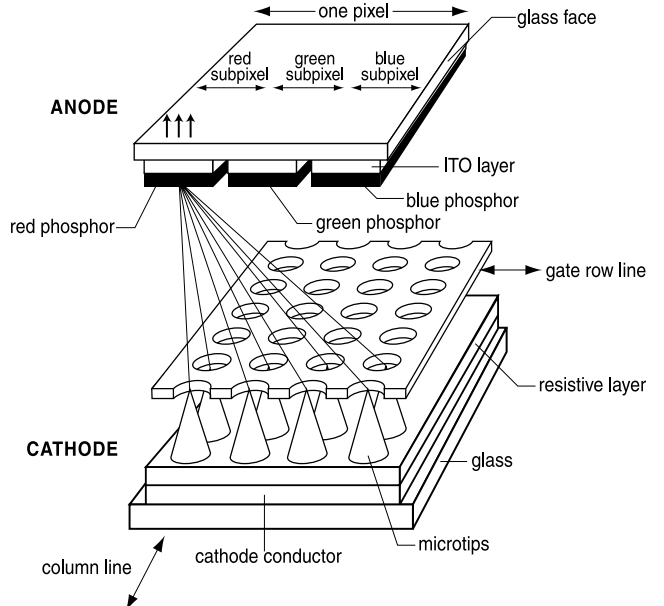


Fig. 5.1: Operation of a field emission display. Reproduced from [14].

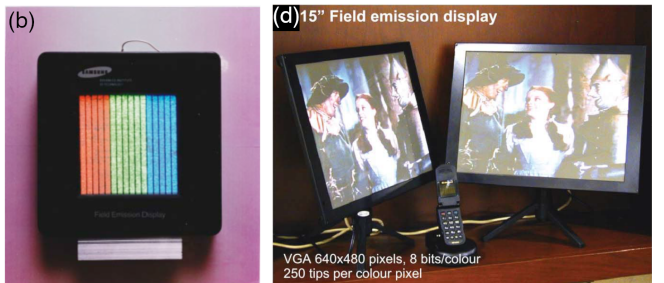


Fig. 5.2: Field emission display prototypes. (a) Sony portable DVD player, adapted from [31]. (b) Samsung 4.5" FED, adapted from [44]. (c) Motorola 4.6" FED, adapted from [46]. (d) Motorola 15" 640 × 480 FEDs and handsets, adapted from [31].

5 Applications of field emission

5.1 Field emission displays

The drive to realise field emission displays was the major impetus for FE research for most of its history. The first US patent for an FED was granted in 1970 [43]; the first working FED prototype was realised in 1986 [14]. The concept was to replace the electron guns in CRT displays with an array of field emitters very close behind the phosphor, which would be addressed as pixels (see fig 5.1). Soon after the first report of CNT field emitters [29], there was significant interest in creating CNT FEDs [44, 45]. Even after reports of early liquid crystal displays (LCDs), FEDs were still perceived to be superior in brightness, response time, contrast, power consumption, and operating temperature range [14]. Commercial companies investing in FED research included, but were not limited to, Samsung, Sony, Motorola, and Philips; a selection of prototypes are shown in fig 5.2.

Ultimately, however, the stability and uniformity issues mentioned in this paper, and manufacturing issues - particularly those related to maintaining a vacuum over a large area - led LCD and LED development to outstrip that of FEDs [10, 14]. All commercial FED research has since shuttered.

Another application for which field emitters have been considered is microwave inductive output amplifiers (IOAs). In these devices, an electron beam, which has been modulated at the cathode by an input RF signal, interacts with (a) a standing wave, in the case of a *klystron*, or (b) a travelling wave, in the case of a *twystrode* to amplify the modulating signal.

Alternatively, the e-beam is not pre-modulated but interacts with the input signal over a longer stretch of waveguide; this is a *travelling-wave tube* (TWT), which does away with the need for a cathode gate [14, 47]. A discussion of the amplification mechanism is far beyond the scope of this work but may be found in [47], for example.

The advantages of FE over thermionic cathodes in this arena are many: the ability to modulate the beam with an electrode very close to the emitter, reducing device size; faster response and thus compatibility with higher frequencies; and lower power consumption [14, 36, 48]. The noise of FE emission presents a relatively small obstacle to IOAs, because it is generally low frequency [14, 49]. A greater concern is the intermittent failure of field emitters, Mo, Si, and CNT based. Although several FE IOA prototypes have been reported [21, 32, 36, 50], more data on lifetimes are needed before FE microwave amplifiers can be commercialised.

5.3 Electron microscopy

As mentioned in 2.2, cold cathode tungsten, a field emitter, is commercially available, and popular, choice of high resolution electron microscopy electron source. A point source is needed for this work [9], so FEAs are unsuitable, but individual CNTs have attracted attention, because they are impervious to the ion sputtering which necessitates such high vacuums for CCW. The current challenge is to reliably attach individual CNTs to a metal tip [10]. There has been some progress in this regard [51], however.

5.4 Other applications

The list of unmentioned potential applications for FE is long, and prospects are better in some areas than others. For brevity, we list the most relevant along with references for the interested reader.

- X-ray generation [52–54]
- Gas ionisation sensors [55, 56]
- Synchrotrons and accelerators [12, 13]
- Space propulsion [57, 58]

6 Conclusion

This review has presented the current state field electron emission technology, paying heed to more popular electron emitters, and to the theory of field emission. The focus has been on carbon nanotubes, as these are the newest and, in some respects, most promising field emitters, but the older Spindt and silicon arrays have been described as well. The most touted potential applications of FE have been outlined, and the suitability of FE analysed for each.

In the author's opinion, FE research and development cannot be separated from the context of commercial interest in display technology. The fact that the rise of LCDs and LEDs have precluded the success of FEDs may well have slowed FE research. Other applications remain where FE has apparent advantages, principally low power and small size, but a lack of understanding of FE noise and intermittent failure, and manufacturing difficulties, are currently the main obstacle to wider commercialisation of field emitters.

References

1. Ossicini, S. & Bertoni, C. M. Image potential at metal surfaces. *Journal of Vacuum Science & Technology A: Vacuum, Surfaces, and Films* **5**, 727–730. issn: 0734-2101. doi:[10.1116/1.574285](https://doi.org/10.1116/1.574285) (July 1987).
2. Jensen, K. L. *Introduction to the physics of electron emission* 1st ed. isbn: 9781119051763 (Wiley, Hoboken, New Jersey, 2017).
3. Li, Y., Sun, Y. & Yeow, J. T. W. Nanotube field electron emission: principles, development, and applications. *Nanotechnology* **26**, 242001. issn: 0957-4484. doi:[10.1088/0957-4484/26/24/242001](https://doi.org/10.1088/0957-4484/26/24/242001) (June 2015).
4. Fowler, R. H. & Nordheim, L. Electron Emission in Intense Electric Fields. *Proceedings of the Royal Society of London. Series A, Containing Papers of a Mathematical and Physical Character* **119**, 173–181. doi:[10.1142/9789814503464_0087](https://doi.org/10.1142/9789814503464_0087) (1928).
5. Jackson, J. D. *Classical electrodynamics* 3rd ed. isbn: 047130932x (Wiley, New York ; Chichester, 1999).
6. Gaertner, G. & Editors, R. G. F. *Modern Developments in Vacuum Electron Sources* (eds Gaertner, G., Knapp, W. & Forbes, R. G.) isbn: 978-3-030-47290-0. doi:[10.1007/978-3-030-47291-7](https://doi.org/10.1007/978-3-030-47291-7) (Springer International Publishing, Cham, 2020).
7. Forbes, R. G. & Deane, J. H. B. Reformulation of the standard theory of Fowler-Nordheim tunnelling and cold field electron emission. *Proceedings of the Royal Society A: Mathematical, Physical and Engineering Sciences* **463**, 2907–2927. doi:[10.1098/rspa.2007.0030](https://doi.org/10.1098/rspa.2007.0030) (2007).

8. Temple, D. *et al.* Silicon field emitter cathodes: Fabrication, performance, and applications. *Journal of Vacuum Science & Technology A: Vacuum, Surfaces, and Films* **16**, 1980–1990. ISSN: 0734-2101. doi:[10.1116/1.581207](https://doi.org/10.1116/1.581207) (May 1998).
9. Ul-Hamid, A. in *A Beginners' Guide to Scanning Electron Microscopy* 15–76 (Springer International Publishing, Cham, 2018). ISBN: 978-3-319-98482-7. doi:[10.1007/978-3-319-98482-7_2](https://doi.org/10.1007/978-3-319-98482-7_2).
10. Cole, M. T., Mann, M., Teo, K. B. K. & Milne, W. I. in *Emerging Nanotechnologies for Manufacturing (Second Edition)* (eds Ahmed, W. & Jackson, M. J.) Second Edi, 125–186 (William Andrew Publishing, Boston, 2015). ISBN: 978-0-323-28990-0. doi:<https://doi.org/10.1016/B978-0-323-28990-0.00005-1>.
11. Hernandez-Garcia, C., Stutzman, M. L. & O'Shea, P. G. Electron sources for accelerators. *Physics Today* **61**, 44–49. ISSN: 00319228. doi:[10.1063/1.2883909](https://doi.org/10.1063/1.2883909) (Feb. 2008).
12. Holland, C., Schwoebel, P., Todd, K., Spindt, C. & Smith, T. *High-speed photo-modulated spindt cathode for FELs in 2013 26th International Vacuum Nanoelectronics Conference, IVNC 2013* (2013). ISBN: 9781467359931. doi:[10.1109/IVNC.2013.6624710](https://doi.org/10.1109/IVNC.2013.6624710).
13. Nichols, K. E. *et al.* Demonstration of transport of a patterned electron beam produced by diamond pyramid cathode in an rf gun. *Applied Physics Letters* **116**, 023502. ISSN: 0003-6951. doi:[10.1063/1.5128109](https://doi.org/10.1063/1.5128109) (Jan. 2020).
14. Zhu, W. *Vacuum Microelectronics* (ed Zhu, W.) ISBN: 047132244X. doi:[10.1002/0471224332](https://doi.org/10.1002/0471224332) (John Wiley & Sons, Inc., New York, USA, Oct. 2001).
15. Dyke, W. P. & Dolan, W. W. in *Advances in Electronics and Electron Physics* (ed Marton, L.) 89–185 (Academic Press, New York, Jan. 1956). doi:[10.1016/S0065-2539\(08\)61226-3](https://doi.org/10.1016/S0065-2539(08)61226-3).
16. Spindt, C. A. A Thin-Film Field-Emission Cathode. *Journal of Applied Physics* **39**, 3504–3505. ISSN: 0021-8979. doi:[10.1063/1.1656810](https://doi.org/10.1063/1.1656810) (June 1968).
17. Spindt, C. A., Holland, C. E., Rosengreen, A. & Brodie, I. Field-Emitter Arrays for Vacuum Microelectronics. *IEEE Transactions on Electron Devices* **38**, 2355–2363. ISSN: 15579646. doi:[10.1109/16.88525](https://doi.org/10.1109/16.88525) (1991).
18. Spindt, C. *A brief history Vacuum Nanoelectronics, the IVNC, and the present status of the Spindt cathode in Technical Digest - 25th International Vacuum Nanoelectronics Conference, IVNC 2012* (2012), 4–5. ISBN: 9781467319812. doi:[10.1109/IVNC.2012.6316876](https://doi.org/10.1109/IVNC.2012.6316876).
19. Spindt, C., Holland, C. & Schwoebel, P. R. Thermal field forming of Spindt cathode arrays. *Journal of Vacuum Science & Technology B, Nanotechnology and Microelectronics: Materials, Processing, Measurement, and Phenomena* **33**, 03C108. ISSN: 2166-2746. doi:[10.1116/1.4904552](https://doi.org/10.1116/1.4904552) (May 2015).
20. Schwoebel, P. R., Spindt, C. A. & Holland, C. E. *High current, high current density field emitter array cathodes* in *Technical Digest of the 17th International Vacuum Nanoelectronics Conference, IVNC 2004* **23** (American Vacuum Society AVS, Apr. 2004), 232. ISBN: 0780383974. doi:[10.1116/1.1849189](https://doi.org/10.1116/1.1849189).
21. Whaley, D. R. *et al.* 100 W operation of a cold cathode TWT. *IEEE Transactions on Electron Devices* **56**, 896–905. ISSN: 00189383. doi:[10.1109/TED.2009.2015614](https://doi.org/10.1109/TED.2009.2015614) (2009).
22. Thomas, R. N. & Nathanson, H. C. Photosensitive field emission from silicon point arrays. *Applied Physics Letters* **21**, 384–386. ISSN: 00036951. doi:[10.1063/1.1654423](https://doi.org/10.1063/1.1654423) (Oct. 1972).
23. Temple, D. Recent progress in field emitter array development for high performance applications. *Materials Science and Engineering R: Reports* **24**, 185–239. ISSN: 0927796X. doi:[10.1016/s0927-796x\(98\)00014-x](https://doi.org/10.1016/s0927-796x(98)00014-x) (Jan. 1999).
24. Xu, N. & Huq, S. E. Novel cold cathode materials and applications. *Materials Science and Engineering: R: Reports* **48**, 47–189. ISSN: 0927796X. doi:[10.1016/j.mser.2004.12.001](https://doi.org/10.1016/j.mser.2004.12.001) (Jan. 2005).
25. Gnade, B. No Title in *Proc. Spring Meeting of the Materials Research Society, Tutorial Program, Symposium G* (San Francisco, C.A., 1997).
26. Yeong, K. S. & Thong, J. T. Life cycle of a tungsten cold field emitter. *Journal of Applied Physics* **99**, 104903. ISSN: 00218979. doi:[10.1063/1.2197267](https://doi.org/10.1063/1.2197267) (May 2006).
27. Lo, W. K. *et al.* Titanium nitride coated tungsten cold field emission sources. *Journal of Vacuum Science & Technology B* **14**, 3787–3791. doi:[10.1116/1.588668](https://doi.org/10.1116/1.588668) (1996).
28. Iijima, S. Helical microtubules of graphitic carbon. *Nature* **354**, 56–58. ISSN: 00280836. doi:[10.1038/354056a0](https://doi.org/10.1038/354056a0) (1991).
29. De Heer, W. A., Châtelain, A. & Ugarte, D. A carbon nanotube field-emission electron source. *Science* **270**, 1179–1180. ISSN: 00368075. doi:[10.1126/science.270.5239.1179](https://doi.org/10.1126/science.270.5239.1179) (Nov. 1995).
30. Sun, Y., Yeow, J. T. W. & Jaffray, D. A. Design and Fabrication of Carbon Nanotube Field-Emission Cathode with Coaxial Gate and Ballast Resistor. *Small* **9**, 3385–3389. ISSN: 16136810. doi:[10.1002/smll.201300553](https://doi.org/10.1002/smll.201300553) (Oct. 2013).
31. Milne, W. I. *et al.* Carbon nanotubes as field emission sources. *Journal of Materials Chemistry* **14**, 933. ISSN: 0959-9428. doi:[10.1039/b314155c](https://doi.org/10.1039/b314155c) (Mar. 2004).
32. Teo, K. B. *et al.* Microwave devices: Carbon nanotubes as cold cathodes. *Nature* **437**, 968. ISSN: 14764687. doi:[10.1038/437968a](https://doi.org/10.1038/437968a) (Oct. 2005).
33. Pirio, G. *et al.* Fabrication and electrical characteristics of carbon nanotube field emission microcathodes with an integrated gate electrode. *Nanotechnology* **13**, 1–4. ISSN: 0957-4484. doi:[10.1088/0957-4484/13/1/301](https://doi.org/10.1088/0957-4484/13/1/301) (Feb. 2002).

34. Li, C. *et al.* Hot electron field emission via individually transistor-ballasted carbon nanotube arrays. *ACS Nano* **6**, 3236–3242. issn: 19360851. doi:[10.1021/nm300111t](#) (Apr. 2012).
35. Chen, G., Shin, D. H., Iwasaki, T., Kawarada, H. & Lee, C. J. Enhanced field emission properties of vertically aligned double-walled carbon nanotube arrays. *Nanotechnology* **19**. issn: 09574484. doi:[10.1088/0957-4484/19/41/415703](#) (Oct. 2008).
36. Minoux, E. *et al.* Carbon nanotube cathodes as electron sources for microwave amplifiers in 2007 7th IEEE International Conference on Nanotechnology - IEEE-NANO 2007, Proceedings (2007), 1248–1251. isbn: 1424406080. doi:[10.1109/NANO.2007.4601409](#).
37. Hirakawa, M., Sonoda, S., Tanaka, C., Murakami, H. & Yamakawa, H. Electron emission properties of carbon nanotubes. *Applied Surface Science* **169**, 662–665. issn: 01694332. doi:[10.1016/S0169-4332\(00\)00808-4](#) (Jan. 2001).
38. Zhu, W., Bower, C., Zhou, O., Kochanski, G. & Jin, S. Large current density from carbon nanotube field emitters. *Applied Physics Letters* **75**, 873–875. issn: 00036951. doi:[10.1063/1.124541](#) (Aug. 1999).
39. Li, Y., Sun, Y., Jaffray, D. A. & Yeow, J. T. A novel field emission microscopy method to study field emission characteristics of freestanding carbon nanotube arrays. *Nanotechnology* **28**, 155704. issn: 13616528. doi:[10.1088/1361-6528/aa613e](#) (Mar. 2017).
40. Dean, K. A. & Chalamala, B. R. Current saturation mechanisms in carbon nanotube field emitters. *Applied Physics Letters* **76**, 375–377. issn: 00036951. doi:[10.1063/1.125758](#) (Jan. 2000).
41. Wang, M., Wang, J. Y., Jin, C., Chen, Q. & Peng, L. M. Observations of Carbon Nanotube Field Emission Failure in the Transmission Electron Microscope. *Materials Science Forum* **475-479**, 4071–4076. issn: 1662-9752. doi:[10.4028/www.scientific.net/MSF.475-479.4071](#) (Jan. 2005).
42. Bonard, J. M., Klinke, C., Dean, K. A. & Coll, B. F. Degradation and failure of carbon nanotube field emitters. *Physical Review B - Condensed Matter and Materials Physics* **67**, 10. issn: 1550235X. doi:[10.1103/PhysRevB.67.115406](#) (Mar. 2003).
43. Crost, M. E., Shoulders, K. & Zinn, M. H. *Thin Electron Tube with Electron Emitters at Intersections of Crossed Conductors* 1970.
44. Choi, W. B. *et al.* Fully sealed, high-brightness carbon-nanotube field-emission display. *Applied Physics Letters* **75**, 3129–3131. issn: 00036951. doi:[10.1063/1.125253](#) (Nov. 1999).
45. Choi, W. *et al.* The First 9-inch Carbon-Nanotube Based Field-Emission Displays for Large Area and Color Applications. *SID Symposium Digest of Technical Papers* **31**. doi:[10.1889/1.1832948](#) (2000).
46. Coll, B. F. *et al.* Nano-emissive display technology for large-area HDTV. *Journal of the Society for Information Display* **14**, 477. issn: 10710922. doi:[10.1889/1.2206113](#) (May 2006).
47. Carter, R. G. *Microwave and RF Vacuum Electronic Power Sources* doi:[10.1017/9780511979231](#) (Cambridge University Press, 2018).
48. Han, J. H. *et al.* Field emission properties of carbon nanotubes grown on Co/TiN coated Ta substrate for cathode in microwave power amplifier. *Diamond and Related Materials* **13**, 987–993. issn: 09259635. doi:[10.1016/j.diamond.2003.11.014](#) (Apr. 2004).
49. Trujillo, J. T., Chakhovskoi, A. G. & Hunt, C. E. Effects of vacuum conditions on low frequency noise in silicon field emission devices in *Proceedings of the IEEE International Vacuum Microelectronics Conference, IVMC 15* (IEEE, Mar. 1996), 133–137. doi:[10.1116/1.589326](#).
50. Li, X. *et al.* Beam Test of a Novel CNT Cathode-Based Electron Gun Assembled in a TWT. *IEEE Transactions on Electron Devices* **66**, 2382–2388. issn: 15579646. doi:[10.1109/TED.2019.2902385](#) (May 2019).
51. Mann, M., Teo, K. B., Milne, W. I. & Tessner, T. Direct Growth of Multi-Walled Carbon Nanotubes on Sharp Tips for Electron Microscopy. *Nano* **01**, 35–39. doi:[10.1142/S1793292006000094](#) (2006).
52. Jeong, J. W. *et al.* A digital miniature x-ray tube with a high-density triode carbon nanotube field emitter. *Applied Physics Letters* **102**. issn: 00036951. doi:[10.1063/1.4776222](#) (Jan. 2013).
53. Parmee, R. J., Collins, C. M., Milne, W. I. & Cole, M. T. *X-ray generation using carbon nanotubes* Dec. 2015. doi:[10.1186/s40580-014-0034-2](#).
54. Li, X. *et al.* Fast microfocus x-ray tube based on carbon nanotube array. *Journal of Vacuum Science & Technology B* **37**, 051203. issn: 2166-2746. doi:[10.1116/1.5099697](#) (Sept. 2019).
55. Choi, I. M. & Woo, S. Y. Application of carbon nanotube field emission effect to an ionization gauge. *Applied Physics Letters* **87**, 1–3. issn: 00036951. doi:[10.1063/1.2112184](#) (Oct. 2005).
56. Li, D. *et al.* Metrological properties of an ionization gauge with carbon nanotube cathode in different gases. *Vacuum* **125**, 222–226. issn: 0042207X. doi:[10.1016/j.vacuum.2016.01.002](#) (Mar. 2016).
57. Kent, B. J., Aplin, K. L., Huq, S. E., Stevens, R. & Wang, L. *Space applications of micro fabricated field emitters* in *Technical Digest of the 18th International Vacuum Nanoelectronics Conference, IVNC 2005* (2005), 82–83. isbn: 0780383974. doi:[10.1109/IVNC.2005.1619495](#).
58. Huo, C., Liang, F. & Sun, A. B. Review on development of carbon nanotube field emission cathode for space propulsion systems. *High Voltage* **5**, 409–415. issn: 23977264. doi:[10.1049/hve.2019.0257](#) (Aug. 2020).